

FATIGUE DAMAGE IN WOOD UNDER PULSATING MULTIAXIAL-COMBINED LOADING

Yasutoshi Sasaki

Associate Professor
Graduate School of Bioagricultural Sciences
Nagoya University
Chikusa, 464-8601 Nagoya, Japan

Mariko Yamasaki

Graduate Student
Graduate School of Engineering
Nagoya Institute of Technology
Showa, 466-8555 Nagoya, Japan

and

Takanori Sugimoto

Graduate Student
Graduate School of Bioagricultural Sciences
Nagoya University
Chikusa, 464-8601 Nagoya, Japan

(Received April 2004)

ABSTRACT

A fatigue test was performed under axial-torsion combined loading, with the aim of investigating fatigue damage in wood under multiaxial stresses. This research particularly focused on the energy loss captured during fatigue tests and the fatigue limit for wood. Air-dried samples of Japanese cypress were used for the tests. An electrohydraulic servomachine that could apply axial and torsional loads simultaneously was used for the fatigue tests. An axial load was applied in the fiber direction (along L), and torque was applied around the axis in the same direction as L. A pulsating triangular axial load was applied in the longitudinal direction at 1 Hz while each specimen was also simultaneously subjected to a twisting moment at the same phase. On the basis of the experimental results of the fatigue tests, energy loss was obtained from the stress-strain curve at each loading cycle and examined precisely in relation to the number of loading cycles and combined stress states. The energy loss per cycle in the dominant stress was large and increased gradually toward fatigue failure. The stress level was so high that the energy loss per cycle was extremely large. In the relationship between cumulative energy loss and the number of loading cycles, the cumulative energy loss was so large that the fatigue life was extremely long. The cumulative energy loss for shear in the compression group was larger than that in the tension group. The mean energy loss per cycle for the fatigue limit was also presumed from the relationships between mean energy loss per cycle, stress amplitude, and fatigue life, and was estimated to be about 10 kJ/m³/cycle, as determined on the basis of the equivalent stress principle. That is, the fatigue life will be infinite when the energy loss per cycle is below 10 kJ/m³/cycle.

Keywords: Fatigue, combined stress, energy loss, fatigue life, fatigue limit.

INTRODUCTION

A component member of a given structure is subjected to a complex stress state in many cases. In addition, structural elements in bridges,

roofs, walls, and floors are intentionally exposed to repeated or reversed cyclic loading situations in service. Therefore, to design a structure more efficiently, it is necessary to fully understand the mechanical behavior of materials under such a

stress state. Many studies on the mechanical behavior of materials, such as concrete, steel, FRP, and bone, under combined stress have been reported (Amijima et al. 1991; Cezayirlioglu et al. 1985; Okajima 1970; Vashishth et al. 2001).

For wood or wood-based materials, much has been reported on their mechanical properties in cases where load, such as compression, tension, or bending, independently acts on them statically and dynamically (Bodig and Jayne 1982; Gong and Smith 2003; Hacker and Ansell 2001; Smith et al. 2003; Thompson et al. 2002). However, there are few studies on the static and dynamic mechanical behavior of wood under multiaxial combined loading in which such loads act on the material simultaneously (Origuchi et al. 1997; Sasaki and Yamasaki 2002, 2004; Yamasaki and Sasaki 2003, 2004). Recently, there has been significant technical development of the timber structure in the fields of civil engineering and construction. Wood is stronger in tension than in compression; thus its fatigue properties are likely to depend on the mode of loading. Understanding the mechanical behavior of wood under combined loading is needed not only in the case of a uniaxial load but also in the case of torsion and axial loads acting simultaneously.

Furthermore, natural materials, such as wood and bone, possess structures fulfilling the requirements for support and the transport of nutrients, and wood has traditionally been regarded as a stereotypical orthotropic material similar to bone. Similarities in function and properties between bone and wood led us to investigate the possible use of wood as an implant material. For example, it is expected that information on the mechanical behavior of wood under combined stress is useful in the development of new composite materials such as artificial bone (Gross and Ezerietis 2003).

Fatigue is the tendency of a material to break, or the process of damage accumulation, under cyclic loading. The fatigue properties of wood and other materials should occupy an important position in structural design. We previously reported the fatigue strength of wood under pulsating tension-torsion combined loading, and discussed the influences of combined-stress

ratio on *S-N* properties and failure mode (Sasaki and Yamasaki 2002). We showed that fatigue strength could be expressed approximately by Hill's criterion for static strength.

In the present research, a rectangular bar of Japanese cypress was used as a test piece, and a fatigue test was performed under combined tension-torsion and compression-torsion. The aim of this paper was to examine energy loss, which was obtained from hysteresis loops trapped throughout a fatigue test, as the response of wood to fatigue under multiaxial stresses.

EXPERIMENTAL METHODS

Sample preparation

The material used in this experiment was Japanese cypress (*Chamaecyparis obtusa* Endl.). Small clear specimens were processed from air-dried lumber samples of the selected timber species. Shape and dimensions of the specimens were the same as in a previous study (Sasaki and Yamasaki 2002). The specimens were cured in the laboratory at 25°C at a relative humidity of 40 %, until the constant weights of the specimens were achieved. The total number of specimens used in all the tests was 161, as shown in Table 1. They were selected based on density to minimize scatter in material quality among the test groups shown in Table 1. The average density and average moisture content were 0.44 ± 0.01 g/cm³ and 7.8 ± 0.3 %, respectively.

Mechanical testing in static

To determine static strength, uniaxial loading, pure torsion, compression-torsion, and tension-torsion combined loading tests were first carried out. Through these tests, the failure surface that which was used as the standard of a fatigue test was obtained. An electrohydraulic servomachine, which could apply axial and torsional loads simultaneously, was used for this study. An axial force was applied in the fiber direction (along L), and torque was applied around the axis in the same direction as L. The procedures for the static loading tests were described pre-

TABLE 1. Number of specimens used in this experiment.

Type of test	Group (Stress state)	Symbol	Number of specimens	Remark
Static tests	Pure compression		5	Results of the static tests are reported in previous study (Sasaki and Yamasaki 2002).
	Combined compression-torsion		12	
	Pure torsion		5	
	Combined tension-torsion		14	
	Pure tension		5	
Fatigue tests	Pure compression	C	7	Two to five specimens were used for each stress level.
	Combined compression-torsion	CC	8	
	Combined compression-torsion	CB	14	
	Combined compression-torsion	CA	12	
	Pure torsion	S	18	
	Combined tension-torsion	TA	15	
	Combined tension-torsion	TB	15	
	Combined tension-torsion	TC	15	
	Pure tension	T	16	

cisely in a previous study (Sasaki and Yamasaki 2002, 2004). The number of specimens for each static test was shown in Table 1.

Failure criterion

The failure surface was obtained by the static tests described above, as a combination of axial and shear strengths. According to the previous study (Sasaki and Yamasaki 2002), it was proved that Hill's criterion approximately expressed the failure condition. In order to determine the combined-stress ratios for fatigue tests under combined loading, Hill's criterion was used.

Based on Hill's criterion normalized by each static strength, combined-stress ratio for the fatigue tests was determined, as schematically shown in Fig. 1; namely, the combined-stress ratio (β) was defined by the ratio of normalized axial stress to the normalized shear stress. Nine β 's, that is, combinations of axial and shear stresses (indicated as C, CC, CB, CA, S, TA, TB, TC, and T) were set up as $\beta = -1:0$ (pure compression, indicated as C), $-0.93:0.38$ (CC), $-0.74:0.71$ (CB), $-0.41:0.92$ (CA), $0:1$ (pure torsion, S), $0.41:0.92$ (TA), $0.73:0.71$ (TB), $0.93:0.38$ (TC), and $1:0$ (pure tension, T), and are shown in Table 2. These β 's equally divided

TABLE 2. Stress ratios and ultimate stresses in axial and shear.

Combined-stress state	Combined-stress ratio (β)		Ultimate stress [MPa]		Remark
	Axial	Shear	Axial (σ_{ult})	Shear (τ_{ult})	
C	1	0	-41.2	0.00	Pure compression
CC	0.93	0.38	-38.2	8.82	Combines compression and shear
CB	0.74	0.71	-30.4	16.7	
CA	0.41	0.92	-16.7	21.6	
S	0	1	0.00	23.5	Pure torsion
TA	0.41	0.92	45.1	21.6	Combined tension and shear
TB	0.73	0.71	81.3	16.7	
TC	0.93	0.38	103	8.82	
T	1	0	111	0.00	Pure tension

Each combined-stress ratio (β) indicates the ratio of stress to pure tensile or pure shear strength, that is, σ_A/F_A or τ_S/F_S , respectively.

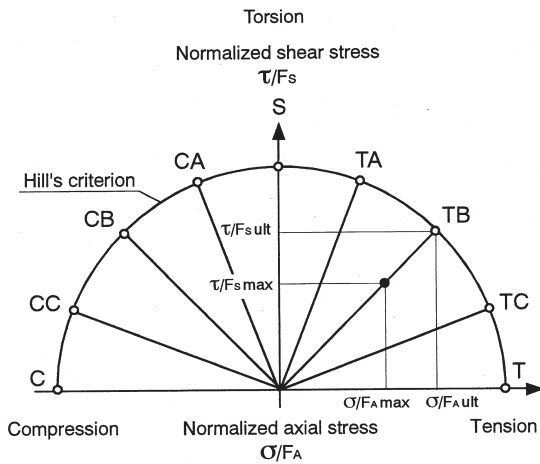


FIG. 1. Schema of Hill's criterion and combined-stress ratios determined for fatigue tests σ is the axial (tensile or compressive) stress, τ is the shear stress, and F_A and F_S are the axial and shear strengths, respectively.

the semicircle of two quadrants for compression-shear and tension-shear combined-stress states into eight based on the failure criterion, as shown in Fig. 1. Each number in Table 2 indicates the ratio of stress to pure axial or shear strength (σ_A/F_A or τ_S/F_S) and the values for each stress combination. As determined from these β 's, the shear stress component was dominant in the combined-stress states CA and TA, and the axial stress component in CC and TC. In the CB and TB states, shear and axial stress components were almost equal.

Mechanical testing in fatigue

The same testing machine used for the static tests was used for the fatigue tests. A pulsating triangular axial (compression or tension) load was applied in the longitudinal direction at 1 Hz while the specimen was also simultaneously subjected to a twisting moment at the same phase, as shown in the previous study (Sasaki and Yamasaki 2002). Stress level in the fatigue tests was determined as the ratio of maximum stress to ultimate stress, whose values are shown in Table 2, and six stages equivalent to 100, 90, 80, 70, 60, and 50 % of these values were determined as the stress levels. For each stress level,

two to five specimens were tested. The total number of specimens used in the fatigue tests was 120, as shown in Table 1. They were selected based on their density to minimize scatter in material quality among the nine test groups shown in Table 1.

The applied axial force and torque, and axial and rotational displacements were measured using the load cells and the electric displacement transducers of the testing machine itself, while longitudinal and shear strain were also measured using strain gages on the LT and LR planes. These data were recorded simultaneously through a dynamic data logger (PCD-1000 manufactured by Kyowa Electronic Instruments Co., Ltd., Tokyo) at a 50 Hz sampling frequency. All the tests were carried out at 25°C at a relative humidity of 40 %.

Failures of the specimens in this study were recognized as follows: tension failure—when the specimen was broken into two parts, compression failure—when the compressive strain was more than 1 % or the failure line was clearly visible at the surface of the specimen, and torsion failure—when the chuck of the testing machine rotated up to $\pi/4$ rad. These standards for failure were based on the results of the mechanical testing under the static condition.

RESULTS AND DISCUSSION

Hysteresis loop capture

Figure 2 shows examples of the stress-strain (S - S) diagrams obtained from the fatigue tests, in which the left panel shows the S - S diagrams in tension and the right panel the S - S diagrams in torsion. As fatigue proceeded, tensile and shear creep occurred under the action of the tensile-torsion fatigue loads, and the hysteresis loops moved along the positive-strain axis. In Fig. 2, for example, the last loops for tension and shear captured before failure had residual strains of about 0.4 and 0.7 %, respectively. The changes in the mechanical properties of wood as a result of fatigue damage are reflected by the changes in the shape of hysteresis loops captured throughout the test. The area within a hysteresis loop is the energy loss per cycle (kJ/m^3). A series of stress versus strain hysteresis loops were captured dur-

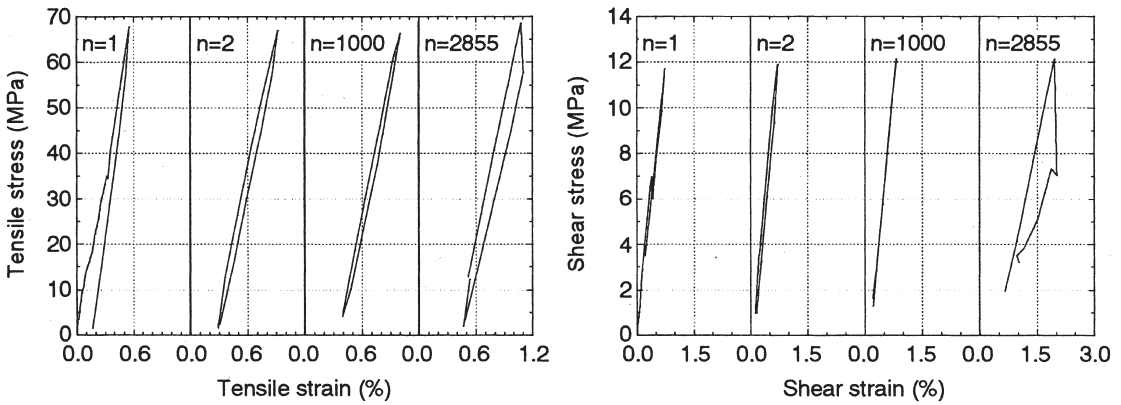


FIG. 2. Examples of stress-strain relationships under pulsating tension-torsion combined loading (combined stress state: TB, stress level: 90%, $N_f = 2855$).

ing a fatigue test, the energy loss was analyzed, and the results are presented in Figs. 3 and 4.

Figures 3 and 4 show the relationship between hysteresis loop area (=energy loss, kJ/m^3) per cycle and the number of loading cycles. Figures 3(a) and (f) show the energy loss per cycle captured by *S-S* diagrams in tension and shear under pure tension and pure torsion fatigue tests, re-

spectively, and Figs. 3(b)–(e) under the tensile-shear combined stress states TC and TA. As shown in Table 2, the tensile-stress component was dominant in the stress state TC and the shear stress component in TA. In Figs. 3(a)–(c), the energy loss per cycle for tensile stress was relatively larger at the beginning of cyclic loading. However, the energy loss per cycle decreased

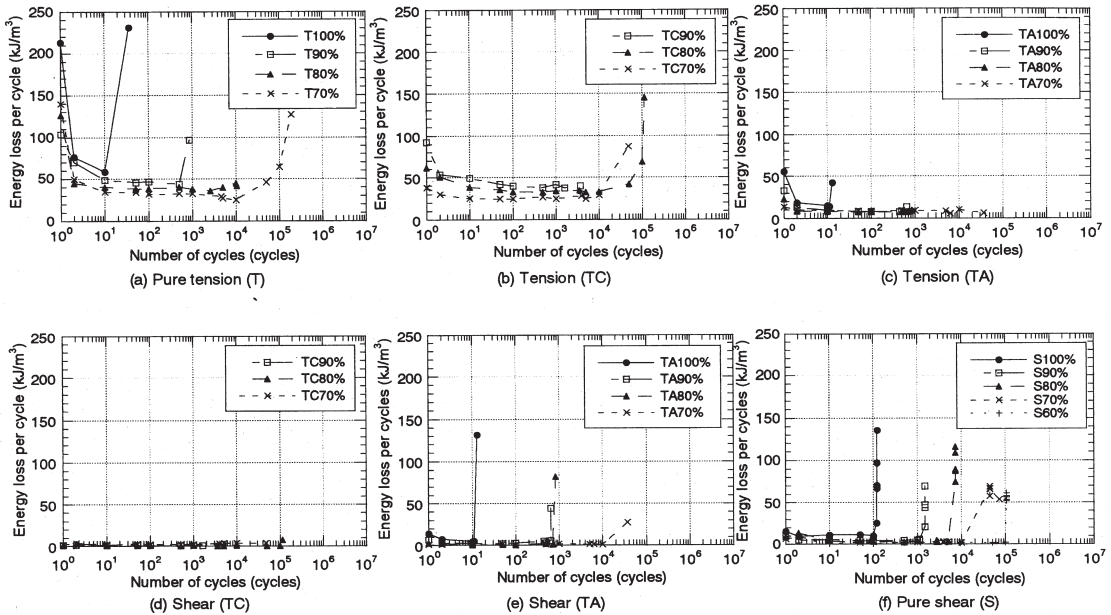


FIG. 3. Relationships between energy loss per cycle and the number of loading cycles obtained from the stress-strain curves in tension and shear.

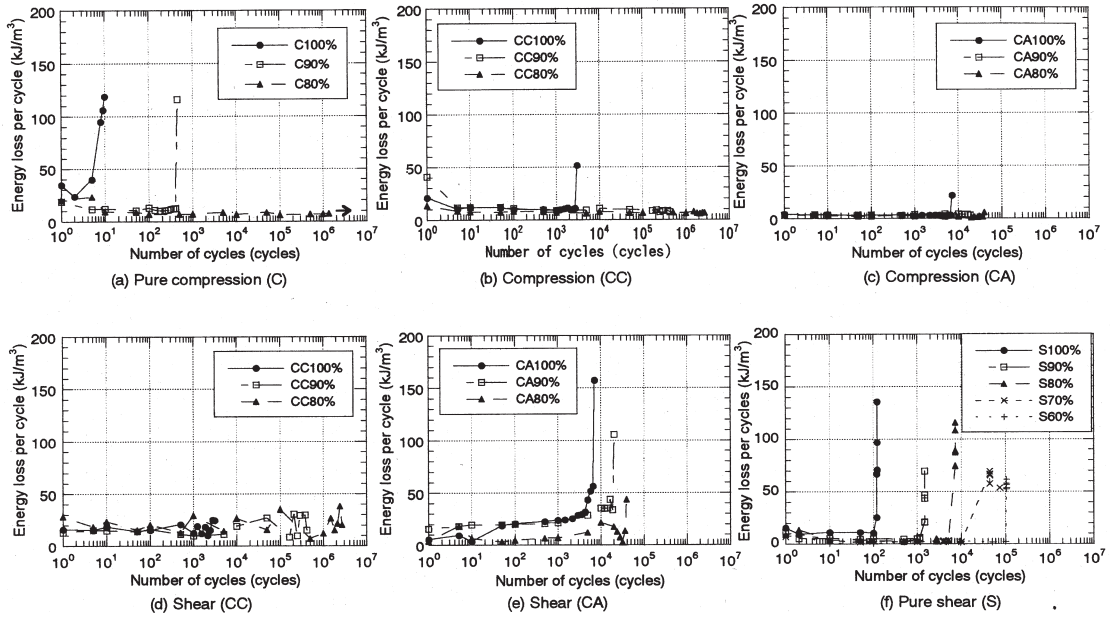


FIG. 4. Relationships between energy loss per cycle and the number of loading cycles obtained from the stress-strain curves in compression and shear.

immediately and was nearly constant after that. It seemed to be under a mechanically unstable state at the first loading, and became under the stable state at the succeeding loading. The energy losses per cycle in T and TC were larger and increased gradually toward fatigue failure, than that in TA, as shown in Figs. 3(a)–(c). It also turned out that the stress level was so high that the energy loss was extremely large. In Fig. 3(d), the energy loss for shear stress was small during fatigue because of the low amplitude of shear stress in TC. Energy loss for shear stress in TA and S increased immediately before fatigue failure, as shown in Figs. 3(e) and (f).

The energy loss per cycle shown in Figs. 4(a) and (f) was captured by *S-S* diagrams in compression and shear under pure compression and pure torsion, respectively, and that in Figs. 4(b)–(e) by the same *S-S* diagrams under the compressive-shear combined stress states CC and CA. The compressive-stress component was dominant in the stress states C and CC and the shear stress component in CA and S. The energy loss for the compressive stress shown in Figs. 4(a)–(c) was relatively smaller than that for the

tensile stress shown in Figs. 3(a)–(c). This is because the compressive-stress amplitude was lower than that of tension, as shown in Table 2. In contrast, the energy loss for shear stress shown in Figs. 4(d) and (e) was larger than that shown in Figs. 3(d) and (e), and the shear stress amplitude was the same in both combined stress states of compressive shear in Fig. 4 and tensile shear in Fig. 3, as shown in Table 2. In addition, the energy loss in CA shown in Fig. 4(e) was larger than that in pure shear shown in Fig. 4(f). This suggests that the energy loss for shear stress is the largest among the compressive-shear combined stress states with little compression. In Figs. 4(e) and (f), energy loss increased sharply immediately before fatigue failure. When the axial or shear stress component was dominant and its amplitude was high, energy loss per cycle for axial or shear stress increased immediately before fatigue failure, as shown in Figs. 3 and 4.

Cumulative energy loss

In the present section, the energy loss per cycle has been accumulated and plotted as a

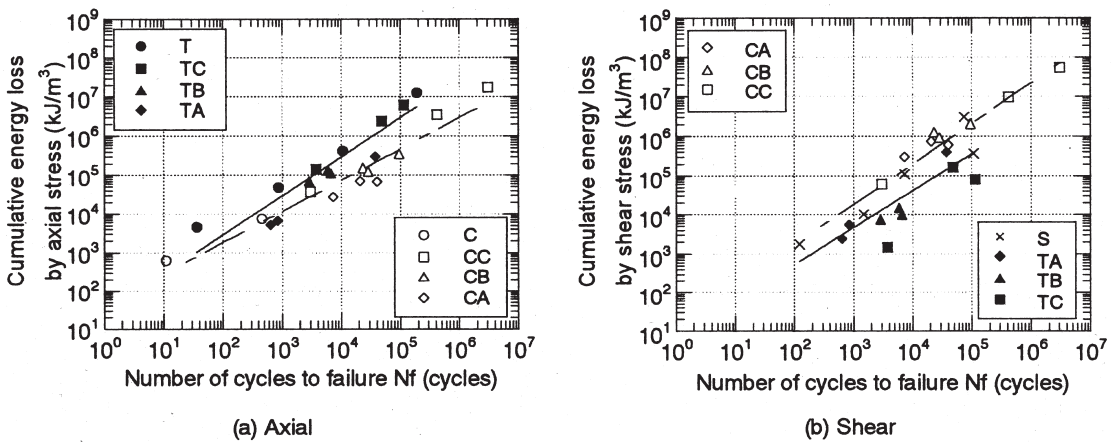


FIG. 5. Relationship between cumulative energy loss and the number of loading cycles to failure.

function of the number of fatigue cycles. The relationship between cumulative energy losses and the number of loading cycles to failure is shown in Fig. 5. The cumulative energy losses shown in Figs. 5(a) and (b) were obtained by the summation of the hysteresis loop areas in axial and shear S - S diagrams, respectively. In both figures, the cumulative energy loss was not constant in relation to the number of cycles to failure. The cumulative energy loss was so large that the fatigue life was extremely long. The cumulative energy loss is in proportion to the fatigue life on double-logarithmic graphs. The values of the cumulative energy loss scattered in a wide range of $10^3 - 10^8 \text{ kJ/m}^3$ in both graphs.

As shown in Fig. 5(a), plots for axial stress in the tension group (T, TC, TB, and TA) are shown in the upper area of the graph. This means that the cumulative energy loss in the tension group is larger than that in the compression group when the fatigue lives in both groups are equal. This is because the tensile stress amplitude was higher than the compressive one, as shown in Table 2. That is, the fatigue life in compression became longer when the cumulative energy losses in both tension and compression groups were equal.

On the other hand, plots for shear stress in the compression group (CA, CB, and CC) are shown in the upper area of the graph, and those in the tension group (TA, TB, and TC) in the lower

area, as shown in Fig. 5(b). Plots for pure shear (S) are shown in the middle. That is, the cumulative energy loss for shear stress under the compressive-shear combined state was larger than that under the tensile-shear combined state. The fatigue life under the tensile-shear combined state was long when the cumulative energy loss under the tensile-shear combined state was the same as that under the compressive-shear combined state. Furthermore, while the values of cumulative energy loss under the compressive-shear combined state scattered in the range of $10^5 - 10^8 \text{ kJ/m}^3$, those under pure shear stress scattered in the range of $10^3 - 10^5 \text{ kJ/m}^3$, which were almost in the same range as those under the tensile-shear combined stresses.

Although the shear stress amplitude was the same in both compression and tension groups, as shown in Table 2, the cumulative energy losses for shear stress differed between these groups. This suggests that the relationships between cumulative energy loss and fatigue life are influenced by β .

Mean energy loss

To consider two S - S relationships in axial (tensile or compressive) and shear stresses synthetically, the equivalent stress principle with which a stress level under multiaxial stress can be converted into a level under uniaxial stress

was introduced. The principle introduced here was derived by von Mises and was expressed as

$$\begin{aligned} \bar{\sigma} &= \sqrt{\sigma^2 + 3\tau^2}, \\ \bar{\varepsilon} &= \sqrt{\varepsilon^2 + \frac{1}{3}\gamma^2}, \end{aligned} \tag{1}$$

where σ and τ are the axial and shear stresses, and ε and γ are the axial and shear strains, respectively. Using Eq. (1), the two *S-S* diagrams in tension and shear shown in Fig. 2 could be unified, and a series of equivalent stress versus equivalent strain hysteresis loops captured during a tension-torsion fatigue test are presented in Fig. 6, for example.

The cumulative energy loss captured during the fatigue tests was also obtained for all the tests and are presented in Fig. 7, as a function of fatigue life. According to the figure, the cumulative energy loss is not constant but increases as fatigue lifetime becomes longer. Figure 7 shows a good correlation between cumulative energy loss and fatigue life on a logarithmic graph, regardless of β ($R=0.95$, 99% significant as reflected by the Spearman's correlation coefficient obtained by a rank test). The cumulative energy losses in the tensile group (TA, TB, TC, and T) were plotted in a slightly upper position than that in the compressive group (CA, CB, CC, and C). This result was

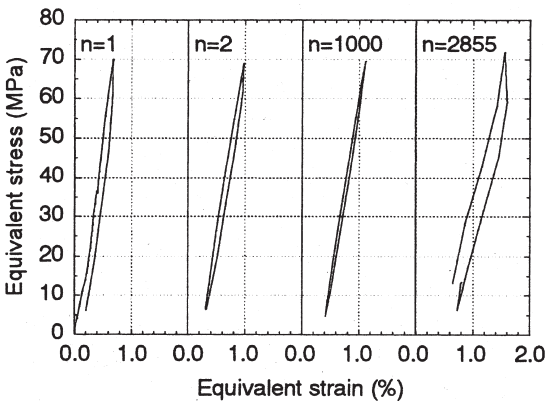


FIG. 6 Series of equivalent stress versus strain hysteresis loops captured during a tension-torsion fatigue tests.

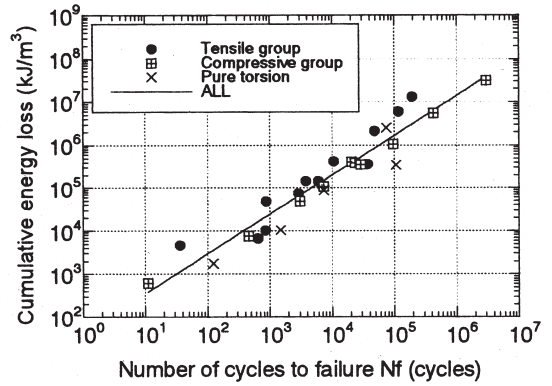


FIG. 7. Relationship between cumulative energy loss and the number of cycles to failure.

due to the absolute value of stress amplitude being larger in tension than in compression because the tensile strength is larger than the compressive strength in the case of wood.

Next, the cumulative energy loss obtained from the equivalent *S-S* relationship was divided by the number of cycles to failure, and it was determined for the mean energy loss per cycle. Figure 8 shows the relationships between the mean energy loss per cycle and the level of equivalent stress. The level of equivalent stress was defined as follows: two individual stresses (axial and shear) were unified to one equivalent stress using Eq. (1), and the equivalent stress was standardized by the maximum value, which was obtained at T-100 % (100 % stress level pure tension). Although the stress level for the fatigue tests in this research was set from 100 to 60 %, the equivalent stress level in Fig. 8 ranged from 100 to 20 %. An exponential distribution is shown in Fig. 8 ($R = 0.83$). According to a previous study on the tensile fatigue of wood (Marsoem et al. 1987), the fatigue limit of wood is presupposed to be about 25 % its strength. The mean energy loss when the stress level is 25 % is about 10 kJ/m³/cycle, reading from the regression line for all data (mean energy loss = $5.03 \cdot e^{-2.86 \text{ equivalent stress level}}$).

Figure 9 shows the relationships between mean energy loss per cycle and fatigue life. The mean energy loss was larger than 10 kJ/m³/cycle, although no notable result is shown in Fig. 9.

This is because the stress levels in the fatigue tests performed in this research were set up higher than the fatigue limit. This suggests that the introduction of the equivalent stress principle here seems reasonable. In a previous study, the mean energy loss per cycle decreased and approached asymptotically constant values as the lifetime lengthened (Okuyama et al. 1984). Roughly speaking, the mean energy loss in Fig. 9 was also seen to gradually approach the fixed value of 10 kJ/m³/cycle. This suggests that if the fatigue limit of wood is 25 % the strength of

wood, the mean energy loss per cycle may be estimated as 10 kJ/m³/cycle.

CONCLUSIONS

From the experimental results of the fatigue tests, energy loss was obtained from the *S-S* diagram at each loading cycle and discussed in relation to fatigue life and fatigue limit. The conclusions drawn are summarized below.

The energy loss per cycle in dominant stress was larger and increased gradually toward fatigue failure. The stress level was so high that the energy loss per cycle was extremely large. The energy loss for shear stress was larger when combined with compression than with tension, although the shear stress amplitude was the same in both compression and tension groups.

In the relationship between cumulative energy loss and the number of loading cycles, the cumulative energy loss was so large that the fatigue life was extremely long. The cumulative energy losses for axial stress in the tension group (T, TC, TB, and TA) were larger than those in the compression group (C, CC, CB, and CA). On the other hand, those for shear in the tension group were smaller than those in the compression group.

The mean energy loss per cycle is also presumed to be about 10 kJ/m³/cycle, considering the relationships between mean energy loss per cycle, fatigue life, and equivalent stress. The fatigue life will be infinite when the energy loss per cycle is below 10 kJ/m³/cycle.

Results obtained in this study would be anticipated as a practical implication in designing a timber construction under a complex stress such as a rigid-frame construction, or also in the development of new composite materials such as artificial bone.

REFERENCES

AMIJIMA , S., T. FUJII, AND M. HAMAGUCHI. 1991. Static and fatigue tests of a woven glass fabric composite under biaxial tension-torsion loading. *Composites* 22:281–289.
 BODIG, J., AND B. A. JAYNE. 1982. *Mechanics of wood and wood composites*. Van Nostrand Reinhold Company, New York, NY. Pp. 394–460.

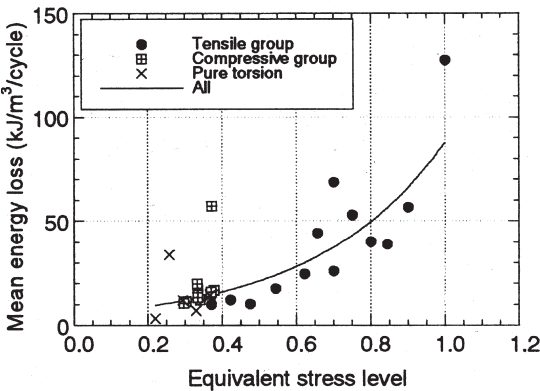


FIG. 8. Relationship between mean energy loss per cycle and stress amplitude.

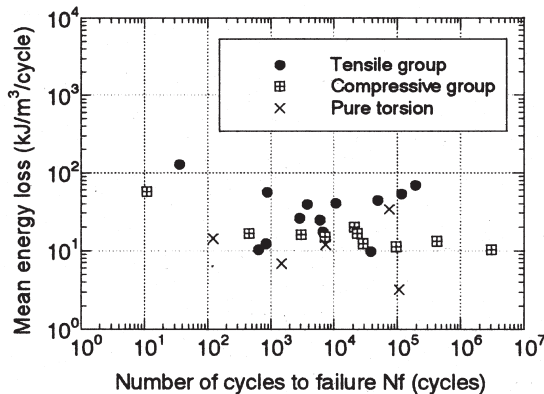


FIG. 9. Relationship between mean energy loss per cycle and the number of cycles to failure.

- CEZAYIRLIOGLU, H., E. BAHNIUK, D. T. DAVY, AND K. G. HEIPLE. 1985. Anisotropic yield behavior of bone under combined axial force and torque. *J. Biomech.* 18:61–69.
- GONG, M., AND I. SMITH. 2003. Effect of waveform and loading sequence on low-cycle compressive fatigue life of spruce. *J. Mater. Civil Eng.* 15:93–99.
- GROSS, K. A., AND E. EZERIETIS. 2003. Juniper wood as a possible implant material. *J. Biomed. Mater. Res.* 64A: 672–683.
- HACKER, C. L., AND M. P. ANSELL. 2001. Fatigue damage and hysteresis in wood-epoxy laminates. *J. Mater. Sci.* 36:609–621.
- MARSOEM, S. N., P.-A. BORDONNÉ, AND T. OKUYAMA. 1987. Mechanical responses of wood to repeated loading II.—Effect of wave form on tensile fatigue. *Mokuzai-Gakkaishi (J. Jpn. Wood Res. Soc.)*. 33:354–360.
- OKAJIMA, T. 1970. Strength of concrete under combined axial force (compression and tension) and torsional moment. *Trans. Architectural Inst. Jpn.* 178:1–8.
- OKUYAMA, T., A. ITOH, AND S. N. MARSOEM. 1984. Mechanical responses of wood to repeated loading I.—Tensile and compressive fatigue fractures. *Mokuzai-Gakkaishi (J. Jpn. Wood Res. Soc.)*. 30:791–798.
- ORIGUCHI, K., H. YOSHIHARA, AND M. OHTA. 1997. Yield behavior of wood under compression-shear combined stress condition. *J. Soc. Mat. Sci. Jpn.* 46:385–389.
- SASAKI, Y. AND M. YAMASAKI. 2002. Fatigue strength of wood under pulsating tension-torsion combined loading. *Wood Fiber Sci.* 34: 508–515.
- , AND ———. 2004. Effect of pulsating tension-torsion combined loading on fatigue behavior in wood. *Holzforschung* 58:666–672.
- SMITH, I., E. LANDIS, AND M. GONG. 2003. *Fracture and fatigue in wood*. John Wiley & Sons Ltd., West Sussex, UK. Pp. 123–154.
- THOMPSON, R. J. H., M. P. ANSELL, P. W. BONFIELD, AND J. M. DINWOODIE. 2002. Fatigue in wood-based panels. Part 1: The strength variability and fatigue performance of OSB, chipboard, and MDF. *Wood Sci. Technol.* 36: 255–269.
- VASHISHTH, D., K. E. TANNER, AND W. BONFIELD. 2001. Fatigue of cortical bone under combined axial-torsional loading. *J. Orthopaedic Res.* 19:414–420.
- YAMASAKI, M. AND Y. SASAKI. 2003. Elastic properties of wood with a rectangular cross section under combined static axial force and torque. *J. Mater. Sci.* 38:603–612.
- , AND ———. 2004. Yield behavior of wood under combined static axial force and torque. *Exp. Mech.* 44: 221–227.